Nat. Hazards Earth Syst. Sci. Discuss., 1, 6521–6557, 2013
www.nat-hazards-earth-syst-sci-discuss.net/1/6521/2013/
doi:10.5194/nhessd-1-6521-2013

Natural Hazards and Earth System Sciences
Discussions
Open Access

Modelling wildland fire propagation by tracking random fronts

G. Pagnini[1,2] **and A. Mentrelli**[3,4]

[1]BCAM – Basque Center for Applied Mathematics, Alameda de Mazarredo 14, 48009 Bilbao, Basque Country, Spain
[2]Ikerbasque, Basque Foundation for Science, Alameda Urquijo 36-5, Plaza Bizkaia, 48011 Bilbao, Basque Country, Spain
[3]Department of Mathematics, University of Bologna, Piazza di Porta San Donato 5, 40126 Bologna, Italy
[4]CIRAM – Research Centre of Applied Mathematics, University of Bologna, via Saragozza 8, 40123 Bologna, Italy

Received: 29 September 2013 – Accepted: 15 October 2013 – Published: 19 November 2013

Correspondence to: G. Pagnini (gpagnini@bcamath.org)

Published by Copernicus Publications on behalf of the European Geosciences Union.

Abstract

Wildland fire propagation is studied in literature by two alternative approaches, namely the reaction-diffusion equation and the level-set method. These two approaches are considered alternative each other because the solution of the reaction-diffusion equation is generally a continuous smooth function that has an exponential decay and an infinite support, while the level-set method, which is a front tracking technique, generates a sharp function with a finite support. However, these two approaches can indeed be considered complementary and reconciled. Turbulent hot-air transport and fire spotting are phenomena with a random character that are extremely important in wildland fire propagation. As a consequence the fire front gets a random character, too. Hence a tracking method for random fronts is needed. In particular, the level-set contourn is here randomized accordingly to the probability density function of the interface particle displacement. Actually, when the level-set method is developed for tracking a front interface with a random motion, the resulting averaged process emerges to be governed by an evolution equation of the reaction-diffusion type. In this reconciled approach, the rate of spread of the fire keeps the same key and characterizing role proper to the level-set approach. The resulting model emerges to be suitable to simulate effects due to turbulent convection as fire flank and backing fire, the faster fire spread because of the actions by hot air pre-heating and by ember landing, and also the fire overcoming a firebreak zone that is a case not resolved by models based on the level-set method. Moreover, from the proposed formulation it follows a correction for the rate of spread formula due to the mean jump-length of firebrands in the downwind direction for the leeward sector of the fireline contour.

1 Introduction

Modelling wildland fire propagation is a twofold challenging task because motivated by social and scientific reasons. In fact, from the social point of view, fire is an hazardous

NHESSD

1, 6521–6557, 2013

Modelling wildland fire propagation

G. Pagnini and A. Mentrelli

phenomenon for human safety and property and also for ecosystems because it can cause its disruption and it is an important source of pollutants (Strada et al., 2012). Moreover, it is a challenging task for scientific reasons because it is a complex phenomenon involving multi-physics and multi-scale processes and it is affected by nonlinear interactions with other Earth processes (Viegas, 1998).

Two different approaches are mainly adopted in literature to investigate wildland fire propagation. One of these modelling approaches is based on evolution equations of the reaction-diffusion type (e.g. Weber et al., 1997; Asensio and Ferragut, 2002; Mandel et al., 2008; Babak et al., 2009) and the other is based on the front traking technique named *level-set method* (Sethian and Smereka, 2003), see for example Mallet et al. (2009), Rehm and McDermott (2009), Mandel et al. (2011).

In a broad sense, diffusion processes are named those small-scale stochastic processes whose displacement at the large scale is governed by a master equation. Diffusion processes are generally driven by parabolic equations, although hyperbolic equations are as well good or even better models for diffusive processes because of the finite front velocity, e.g. the telegraph equation. When a source term is added, the resulting equation is termed reaction-diffusion equation. Hence, reaction-diffusion equations model the propagation of a reacting interface embedded in a random environment. This type of equations embody a very general mathematical model that can be applied to several phenomena.

What concerns the level-set method, in general it is particularly useful to handle problems in which the speed of an evolving interface is dependent on the interface properties such as curvature and normal direction, as well as on the boundary conditions at the interface location. Hence, it is suitable for problems in which the topology of the evolving interface changes during the events and for problems in which sharp corners and cusps can be generated (Sethian and Smereka, 2003).

These approaches are considered alternative each other because of the different behaviour of their solutions. In particular, the solution of the reaction-diffusion equation is generally a continuous smooth function that has an exponential decay and an infinite support while the solution obtained by the level-set method is a sharp function with a finite support. However, these two approaches can indeed be considered complementary and reconciled.

In fact, extremely important phenomena in wildland fire propagation are turbulent hot-air transport due to the turbulent nature of the Atmospheric Boundary Layer and consequentely to the fire-atmosphere interactions (Clark et al., 1996; Potter, 2002, 2012a, b; Linn and Cunningham, 2005; Cunningham and Linn, 2007; Sun et al., 2006; Clements et al., 2008; Filippi et al., 2009, 2011, 2013; Sun et al., 2009; Mandel et al., 2011; Forthofer and Goodrick, 2011), as well as the fire spotting phenomenon (Sardoy et al., 2007, 2008; Kortas et al., 2009; Perryman, 2009; Koo et al., 2010; Wang, 2011; Morgante, 2011; Perryman et al., 2013). Both processes have a random character, thefore the fire front motion turns to be random. Different stochastic approches have been proposed in literature (see e.g. Favier, 2004; Hunt, 2007; Boychuk et al., 2009; Almeida and Macau, 2011; Perryman et al., 2013). Here, the level-set method for tracking fronts is extended to track random fronts. The frontline motion is randomized by summing to the motion in the outward normal direction, whose intensity is determined by the so-called rate of spread (ROS), two noises corresponding to turbulent transport and fire spotting. The resulting averaged process emerges to be governed by an evolution equation of the reaction-diffusion type and the ROS drives the source term. Actually, the randomization of the fireline contour is performed according to the probability density function (PDF) of the front particle displacement and the ROS of the fire keeps the same key and characterizing role proper to the level-set approach. When the random motion turns to be deterministic, the reaction-diffusion equation reduces to the Hamilton–Jacobi equation typical of the level-set method.

The resulting model emerges to be suitable to simulate effects due to turbulent convection as flanking and backing fire, the faster fire spread because of the pre-heating action by the hot air and of the ember landing, and also the fire overcoming a firebreak zone that is a case not resolved by models based on the level-set method. Moreover, a correction for the ROS formula is also obtained which includes the effect by the mean jump-length of firebrands in the leeward sector of the fireline contour and by the mean wind.

The paper is organized as follows. In Sect. 2 the approaches based on the reaction-diffusion equation and the level-set method for wildland fire propagation are briefly reminded. In Sect. 3 a picture to model wildland fire propagation is depicted and the mathematical formulation of a method for tracking random fronts is introduced. In Sect. 4 the proposed model is discussed and in Sect. 5 results from numerical simulations are shown. Finally in Sect. 6 conclusions are reported.

2 Reaction-diffusion equations and level-set method in wildland fire propagation

2.1 Reaction-diffusion equation modelling

An important observable for fire mapping is the temperature field. Actually, temperature is spread by molecular processes and turbulent flows so it has a random character and is modelled by a diffusion process. Furthermore, the fire is an energy source and a reaction-diffusion equation follows from conservation of energy and fuel on the basis of combustion waves approach (Weber et al., 1997). Two-equation models concerning the average temperature field $T(\boldsymbol{x},t)$ and the fuel mass fraction $Y(\boldsymbol{x},t)$, $Y \in [0,1]$, have been developed and analyzed in literature (see e.g. Montenegro et al., 1997; Asensio and Ferragut, 2002; Serón et al., 2005; Mandel et al., 2008; Babak et al., 2009). In a highly simplified form, these models read

$$\frac{\partial T}{\partial t} + \boldsymbol{U}\,\nabla T = K\,\nabla^2 T + \frac{Q}{c_\mathrm{p}} R\,Y - \frac{h\,A}{\rho\,c_\mathrm{p} V}(T - T_\mathrm{a})\,, \tag{1a}$$

$$\frac{\partial Y}{\partial t} = -R\,Y\,, \quad T > T_\mathrm{a}\,, \tag{1b}$$

NHESSD

1, 6521–6557, 2013

Modelling wildland fire propagation

G. Pagnini and A. Mentrelli

where $\boldsymbol{U}$ is the mean wind velocity, K the diffusion coefficient, Q the heat of reaction, c_p the specific heat of fuel, R the reaction rate, h the heat transfer coefficient from fuel to surroundings, ρ the density of fuel, A/V the surface area to volume ratio for fuel configuration and T_a the ambient temperature. This approach has been also calibrated, validated and implemented in a data assimilation system (Mandel et al., 2008). Further reaction-diffusion models for wildland fire propagation have been reviewed by Sullivan (2009).

However, in order to represent the burned/unburned front, reaction–diffusion equations have been developed whose solutions are sharp waves almost constant elsewhere except in the interface region. Concerning this, since the level-set method (Sethian and Smereka, 2003), which is a front tracking technique, generates bi-value sharp solutions with finite support it emerges to be the other widely used approach for modelling wildland fire propagation (Beezley et al., 2008; Rehm and McDermott, 2009; Mallet et al., 2009; Mandel et al., 2009; Dobrinkova et al., 2011; Mandel et al., 2011; Coen et al., 2013).

2.2 General formulation of the level-set method

The level-set method can be briefly described as follows. Let Γ be a simple closed curve, or an ensemble of simple non-intersecting closed curves, representing a propagating interface in two dimensions, and let $\gamma : \mathcal{S} \times [0,+\infty[\to \mathbb{R}$ be a function defined on the domain of interest $\mathcal{S} \subseteq \mathbb{R}^2$ such that the level-set γ_*, i.e. $\gamma(\boldsymbol{x},t) = \gamma_*$, coincides with the evolving front, i.e. $\Gamma(t) = \{\boldsymbol{x} \in \mathcal{S} \mid \gamma(\boldsymbol{x},t) = \gamma_*\}$. In the case of Γ being an ensemble of n curves, the ensemble of the n interfaces is considered as *interface*.

The evolution of the field γ is governed by an Hamilton–Jacobi equation, which reads as follows:

$$\frac{D\gamma}{Dt} = \frac{\partial \gamma}{\partial t} + \frac{\mathrm{d}\boldsymbol{x}}{\mathrm{d}t} \cdot \nabla \gamma = 0 , \quad \gamma(\boldsymbol{x}, t = 0) = \gamma_0(\boldsymbol{x}) , \tag{2}$$

where γ_0 is the initial field embedding the interface Γ at $t = 0$, $\Gamma_0 \equiv \Gamma(t = 0)$.

NHESSD
1, 6521–6557, 2013

If the motion of the interface is directed towards the outward normal $\hat{\boldsymbol{n}} = -\nabla\gamma/\|\nabla\gamma\|$, i.e.

$$\frac{d\boldsymbol{x}}{dt} = \boldsymbol{V}(\boldsymbol{x},t) = \mathcal{V}(\boldsymbol{x},t)\,\hat{\boldsymbol{n}}\,, \tag{3}$$

then Eq. (2) becomes

$$\frac{\partial\gamma}{\partial t} = \mathcal{V}(\boldsymbol{x},t)\|\nabla\gamma\|\,, \tag{4}$$

which is the *ordinary* level-set equation, and $\gamma(\boldsymbol{x},t)$ can be named *level-set function*.

2.3 Application of the level-set method to the wildland fire propagation

Within the formalism introduced in Sect. 2.2, the subsets of the domain $\mathcal{S}$ corresponding to the interface Γ and to the region Ω enclosed by Γ (which represent, respectively, the fireline and the burnt area) may be conveniently identified as the positive-valued regions selected by the two indicator functions $\mathcal{I}_\Gamma, \mathcal{I}_\Omega : \mathcal{S} \times [0,+\infty[\rightarrow \{0,1\}$ defined as follows:

$$\mathcal{I}_\Gamma(\boldsymbol{x},t) = \begin{cases} 1\,, & \text{if } \gamma(\boldsymbol{x},t) = \gamma_* \\ 0\,, & \text{elsewhere} \end{cases}\,, \tag{5}$$

and

$$\mathcal{I}_\Omega(\boldsymbol{x},t) = \begin{cases} 1\,, & \text{if } \gamma(\boldsymbol{x},t) \le \gamma_* \\ 0\,, & \text{elsewhere} \end{cases}\,. \tag{6}$$

The indicator functions at time $t = 0$, i.e. $\mathcal{I}_\Gamma(\boldsymbol{x},t=0)$ and $\mathcal{I}_\Omega(\boldsymbol{x},t=0)$, describing the initial topology of the fire, are indicated in the following as $\mathcal{I}_{\Gamma_0}(\boldsymbol{x})$ and $\mathcal{I}_{\Omega_0}(\boldsymbol{x})$, respectively.

NHESSD
1, 6521–6557, 2013

In the case of a fireline Γ made of more than one closed curve, the domain Ω is not simply connected, resulting in more than one burnt areas independently evolving.

When the application to wildland fire propagation is considered, the quantity $\mathcal{V}(\boldsymbol{x}, t)$, which has the dimension of a velocity, is identified by the ROS. The ROS value essentially depends on environmental conditions, i.e. intensity and direction of the wind and the orography of the terrain, and on the fuel conditions, i.e. type and characteristics of the vegetation. Several determinations of the ROS have been proposed in literature, some are based on experimental data and others on certain physical insight (see e.g. Rothermel, 1972; Finney, 2002, 2003; Balbi et al., 2007, 2009; Mallet et al., 2009).

Finally, instead of physically based differential equations, empirically observed properties of the fire such as the ROS can be used to model fireline evolution. In this regard, empirical or physical based formulae for the ROS can be straightforwardly included into the level-set method. Data assimilation (Mandel et al., 2009) has been considered also for the level-set approach and more it has been implemented into coupled weather-wildland fire models (Mandel et al., 2009, 2011; Coen et al., 2013).

3 Model picture and mathematical formulation of a method for tracking random fronts

The approach derived in this section is an improvement of the approach originally formulated for a Lagrangian description of turbulent premixed combustion (Pagnini and Bonomi, 2011), and later extended to the study of wildland fire propagation including the effects of turbulence (Pagnini and Massidda, 2012, 2013). Here, the latter model is further developed in order to include fire spotting phenomena.

Let a large number of *potential* flame holders be distributed over the surface S covered by the fuel. Before the fire starts, each one of these *potential* flame holders stays at rest with a switched off torch. When the fire starts, the torches of some potential flame holders are switched on, so that they turn into *active* flame holders; the locus of these initial *active* flame holders is the fireline Γ_0.

The *active* flame holders start to move with their burning torches. After a while, when an *active* flame holder reaches a *potential* flame holder, the latter turns into an *active* flame holder, too. As a consequence, the number of the active flame holders and the length of the fireline Γ increase in time. However, the growing process of the fireline length, $\mathcal{L}(t)$, and that of the number of *active* flame holders, $\mathcal{N}(t)$, are strongly dependent. In fact, when the length of the fireline grows, also the number of the *active* flame holder increases, because the fireline contour can grow solely if a new *potential* flame holder turns into an *active* flame holder. To conclude, the growing ratio of the fireline, i.e. $\mathcal{L}(t)/\mathcal{L}(0)$, and that of the number of the *active* flame holders, i.e. $\mathcal{N}(t)/\mathcal{N}(0)$, are equal. Hence, to each *active* flame holder, it can be associated a constant *action arc-length* $d = \mathcal{L}(t)/\mathcal{N}(t) = \mathcal{L}(0)/\mathcal{N}(0)$.

The above argoument based on the ideas of *active* flame holders and constant *action arc-length* can be compared with the concepts of Lagrangian markers and constant fire-perimeter resolution introduced in the front tracking method discussed by Filippi et al. (2010, 2013).

Let the motion of each *active* flame holder be random, e.g. due to turbulence and fire spotting effects. For any realization indexed by ω, the random trajectory of each *active* flame holder is stated to be $\boldsymbol{X}^{\omega}(t,\overline{\boldsymbol{x}}_0)$ with the same fixed initial condition $\boldsymbol{X}^{\omega}(0,\overline{\boldsymbol{x}}_0) = \overline{\boldsymbol{x}}_0$ in all realizations.

By using statistical mechanics formalism (Klimontovich, 1994), the trajectory of a single *active* flame holder is marked out by the one-particle density function $f^{\omega}(\boldsymbol{x};t) = \delta(\boldsymbol{x} - \boldsymbol{X}^{\omega}(t,\overline{\boldsymbol{x}}_0))$, where $\delta(\boldsymbol{x})$ is the Dirac δ-function.

Observing that in the deterministic case the level-set function γ solution of Eq. (4) may be written as

$$\gamma(\boldsymbol{x},t) = \int_{\mathcal{S}} \gamma\left(\overline{\boldsymbol{x}},t\right)\, \delta\left(\boldsymbol{x} - \overline{\boldsymbol{x}}\right)\, d\overline{\boldsymbol{x}}, \tag{7}$$

the effects of randomness are incorporated in the model assuming that, in the ϖ-realization, the level-set function γ^{ϖ} embedding the fireline Γ^{ϖ} is obtained as a straightforward generalization of Eq. (7) as follows:

$$\gamma^{\varpi}(\boldsymbol{x},t) = \int_{\mathcal{S}} \gamma(\overline{\boldsymbol{x}},t)\,\delta(\boldsymbol{x}-\boldsymbol{X}^{\varpi}(t,\overline{\boldsymbol{x}}))\,d\overline{\boldsymbol{x}}\,. \tag{8}$$

Accordingly, $\mathcal{I}_{\Gamma}$ and $\mathcal{I}_{\Omega}$ are replaced by the new indicator functions $\mathcal{I}_{\Gamma^{\varpi}},\mathcal{I}_{\Omega^{\varpi}} : \mathcal{S}\times[0,+\infty[\,\longrightarrow\{0,1\}$ defined as follows:

$$\begin{aligned}
\mathcal{I}_{\Gamma^{\varpi}}(\boldsymbol{x},t) &= \int_{\mathcal{S}} \mathcal{I}_{\Gamma_0}(\overline{\boldsymbol{x}}_0)\,\delta(\boldsymbol{x}-\boldsymbol{X}^{\varpi}(t,\overline{\boldsymbol{x}}_0))\,d\overline{\boldsymbol{x}}_0 \\
&= \int_{\Gamma_0} \delta(\boldsymbol{x}-\boldsymbol{X}^{\varpi}(t,\overline{\boldsymbol{x}}_0))\,d\overline{\boldsymbol{x}}_0 \\
&= \int_{\Gamma(t)} \delta(\boldsymbol{x}-\boldsymbol{X}^{\varpi}(t,\overline{\boldsymbol{x}}))\,d\overline{\boldsymbol{x}}\,,
\end{aligned} \tag{9}$$

and

$$\begin{aligned}
\mathcal{I}_{\Omega^{\varpi}}(\boldsymbol{x},t) &= \int_{\mathcal{S}} \mathcal{I}_{\Omega_0}(\overline{\boldsymbol{x}}_0)\,\delta(\boldsymbol{x}-\boldsymbol{X}^{\varpi}(t,\overline{\boldsymbol{x}}_0))\,d\overline{\boldsymbol{x}}_0 \\
&= \int_{\Omega_0} \delta(\boldsymbol{x}-\boldsymbol{X}^{\varpi}(t,\overline{\boldsymbol{x}}_0))\,d\overline{\boldsymbol{x}}_0 \\
&= \int_{\Omega(t)} \delta(\boldsymbol{x}-\boldsymbol{X}^{\varpi}(t,\overline{\boldsymbol{x}}))\,d\overline{\boldsymbol{x}}\,,
\end{aligned} \tag{10}$$

NHESSD
1, 6521–6557, 2013

where, for any fixed initial condition $\overline{\boldsymbol{x}}_0$, the evolution of the deterministic trajectory is noted by $\overline{\boldsymbol{x}}(t)$ and it is uniquely obtained by a deterministic time-reversible map $\overline{\boldsymbol{x}}(t) = \mathcal{F}(t, \overline{\boldsymbol{x}}_0)$. Moreover, the assumption of a constant arc-length of action implies a constant density of flame holders along the fireline, from which an incompressibility-like condition follows and then $J = d\overline{\boldsymbol{x}}_0 / d\overline{\boldsymbol{x}} = 1$.

Hence, denoting by $\langle \cdot \rangle$ the ensemble average, the *effective indicator* of the burnt region, $\varphi_e(\boldsymbol{x}, t) : \mathcal{S} \times [0, +\infty[\to [0, 1]$, may be defined as:

$$\begin{aligned} \varphi_e(\boldsymbol{x}, t) = \langle \mathcal{I}_{\Omega^\omega(t)} \rangle &= \left\langle \int_{\Omega(t)} \delta(\boldsymbol{x} - \boldsymbol{X}^\omega(t, \overline{\boldsymbol{x}}))\, d\overline{\boldsymbol{x}} \right\rangle \\ &= \int_{\Omega(t)} \langle \delta(\boldsymbol{x} - \boldsymbol{X}^\omega(t, \overline{\boldsymbol{x}})) \rangle\, d\overline{\boldsymbol{x}} \\ &= \int_{\Omega(t)} f(\boldsymbol{x}; t | \overline{\boldsymbol{x}})\, d\overline{\boldsymbol{x}}, \end{aligned} \tag{11}$$

where $f(\boldsymbol{x}; t | \overline{\boldsymbol{x}}) = \langle \delta(\boldsymbol{x} - \boldsymbol{X}^\omega(t, \overline{\boldsymbol{x}})) \rangle$ is the PDF of the displacement of the *active* flame holders around the average position $\overline{\boldsymbol{x}}$. Equation (11) has been originally proposed to model the burned mass fraction in turbulent premixed combustion (Pagnini and Bonomi, 2011).

It should be noted that the *effective indicator* φ_e introduced here is not an indicator function in the classical sense. In fact, adopting the language of fuzzy logic, it is properly a *membership function*, being its range the compact interval $[0, 1]$ rather than the discrete set $\{0, 1\}$. Despite this, since the concept of probability which led to Eq. (11) should not be confused with the concept of degree of truth (typical of fuzzy logic), φ_e is classify as an indicator function instead of a membership function.

NHESSD
1, 6521–6557, 2013

Making use of the indicator function $\mathcal{I}_\Omega$, Eq. (11) can be further written as:

$$\varphi_e(\boldsymbol{x},t) = \int_{\mathcal{S}} \mathcal{I}_\Omega(\overline{\boldsymbol{x}},t)\, f(\boldsymbol{x};t|\overline{\boldsymbol{x}})\, d\overline{\boldsymbol{x}}. \tag{12}$$

It is worth noting that the deterministic trajectory $\overline{\boldsymbol{x}}$ is the trajectory of a point belonging to the ordinary level-set contour with the same initial condition $\overline{\boldsymbol{x}}_0$. In the deterministic case, i.e. $\boldsymbol{X}^{\omega}(t,\overline{\boldsymbol{x}}) = \overline{\boldsymbol{x}}$ for all realizations, it turns out that $f(\boldsymbol{x};t|\overline{\boldsymbol{x}}) = \delta(\boldsymbol{x} - \overline{\boldsymbol{x}})$, and from Eq. (12) it is recovered $\varphi_e(\boldsymbol{x},t) = \mathcal{I}_{\Omega(t)}$.

It may also be noted that Eq. (12) is remarkably close to the formulation found in Smoothed Particle Hydrodynamics (SPH) theory (Monaghan, 2005); nonetheless in the present approach the choice of the kernel function and that of the smoothing length are removed because they straightforwardly follow from the PDF $f(\boldsymbol{x};t|\overline{\boldsymbol{x}})$.

Applying the Reynolds transport theorem to Eq. (11), the evolution equation of the effective indicator $\varphi_e(\boldsymbol{x},t)$ reads as (Pagnini and Bonomi, 2011):

$$\frac{\partial \varphi_e}{\partial t} = \int_{\Omega(t)} \frac{\partial f}{\partial t}\, d\overline{\boldsymbol{x}} + \int_{\Omega(t)} \nabla_{\overline{\boldsymbol{x}}} \cdot [\boldsymbol{V}(\overline{\boldsymbol{x}},t)\, f(\boldsymbol{x};t|\overline{\boldsymbol{x}})]\, d\overline{\boldsymbol{x}}. \tag{13}$$

Taking into account that $f(\boldsymbol{x};t|\overline{\boldsymbol{x}})$ satisfies the evolution equation

$$\frac{\partial f}{\partial t} = \mathcal{E} f, \tag{14}$$

where $\mathcal{E} = \mathcal{E}(\boldsymbol{x})$ is a generic evolution operator not acting on $\overline{\boldsymbol{x}}$ and t, Eq. (13) can be written as:

$$\frac{\partial \varphi_e}{\partial t} = \mathcal{E}\varphi_e + \int_{\Omega(t)} \nabla_{\overline{\boldsymbol{x}}} \cdot [\boldsymbol{V}(\overline{\boldsymbol{x}},t)\, f(\boldsymbol{x};t|\overline{\boldsymbol{x}})]\, d\overline{\boldsymbol{x}}. \tag{15}$$

NHESSD
1, 6521–6557, 2013

To conclude, let $\kappa(\overline{\boldsymbol{x}},t)$ be the mean front curvature defined by $\kappa(\overline{\boldsymbol{x}},t) = \nabla_{\overline{\boldsymbol{x}}} \cdot \hat{\boldsymbol{n}}/2$. Since the fireline velocity with intensity given by the ROS is actually a function of the curvature, rather than the position, i.e. $\boldsymbol{V} = \boldsymbol{V}(\kappa,t) \equiv \mathcal{V}(\kappa,t)\,\hat{\boldsymbol{n}}$, the evolution equation of $\varphi_{\mathrm{e}}(\boldsymbol{x},t)$ becomes

$$\frac{\partial \varphi_{\mathrm{e}}}{\partial t} = \mathcal{E}\,\varphi_{\mathrm{e}} + \int_{\Omega(t)} \boldsymbol{V} \cdot \nabla_{\overline{\boldsymbol{x}}} f \; d\overline{\boldsymbol{x}} + \int_{\Omega(t)} f \left\{ \frac{\partial \mathcal{V}}{\partial \kappa} \nabla_{\overline{\boldsymbol{x}}} \kappa \cdot \hat{\boldsymbol{n}} + 2\mathcal{V}(\kappa,t)\,\kappa(\overline{\boldsymbol{x}},t) \right\} d\overline{\boldsymbol{x}} \,. \tag{16}$$

Equation (16) is a reaction-diffusion type equation that is associated to the level-set equation (4). The fireline propagation is thus affected, in the present model, by: the ROS, i.e. $\boldsymbol{V}(\overline{\boldsymbol{x}},t) = \mathcal{V}(\boldsymbol{x},t)\,\hat{\boldsymbol{n}}$; the mean front curvature, i.e. $\kappa(\overline{\boldsymbol{x}},t)$; the turbulent dispersion and the fire spotting phenomenon, both modelled by means of a single PDF, i.e. $f(\boldsymbol{x};t|\overline{\boldsymbol{x}})$.

It is here highlighted that this formulation holds for any determination of the ROS (see e.g. Rothermel, 1972; Finney, 2002, 2003; Balbi et al., 2007, 2009; Mallet et al., 2009). For a deterministic motion, i.e. when $f(\boldsymbol{x};t|\overline{\boldsymbol{x}}) = \delta(\boldsymbol{x}-\overline{\boldsymbol{x}})$, Eq. (16) reduces to the ordinary level-set equation 4 (Pagnini and Bonomi, 2011).

Since, as previously pointed out, the range of the effective indicator φ_{e} is the compact interval $[0,1]$, a criterion to mark the *effective* burned region Ω_e has to be stated. The choice here is to mark as burned the region in which the effective indicator exceeds an arbitrarily fixed threshold value $\varphi_{\mathrm{e}}^{\mathrm{th}}$, i.e. $\Omega_e(\boldsymbol{x},t) = \{\boldsymbol{x} \in \mathcal{S} \mid \varphi_{\mathrm{e}}(\boldsymbol{x},t) > \varphi_{\mathrm{e}}^{\mathrm{th}}\}$. However, beside this criterion, a further criterion associated to an ignition delay due to the pre-heating action of the hot air or to the landing of firebrands should be introduced. This ignition delay was previously considered as an heating-before-burning mechanism due to the hot air (Pagnini and Massidda, 2012, 2013). Actually it can be generalized to include fire spotting.

The ignition delay can be understood as an electrical resistance. Since the fuel can burn because of two pathways, i.e. hot-air heating and firebrand landing, the resistance analogy suggests that the resulting ignition delay can be approximatively computed as resistances acting in parallel. Hence, let τ_h and τ_f be the ignition delay due to hot air and firebrands, respectively, the joint ignition delay τ is

$$\frac{1}{\tau} = \frac{1}{\tau_\mathrm{h}} + \frac{1}{\tau_\mathrm{f}} = \frac{\tau_\mathrm{h} + \tau_\mathrm{f}}{\tau_\mathrm{h}\,\tau_\mathrm{f}} . \tag{17}$$

The ignition delay associated to firebrands is in general much smaller than that associated to hot air because embers burn by contact, hence $\tau_\mathrm{h} \gg \tau_\mathrm{f}$ so that it holds $\tau \simeq \tau_\mathrm{f}$. Finally, the heating-before-burning mechanism is depicted as the persistence in time of the effective fire front, i.e.

$$\psi(\boldsymbol{x},t) = \int_0^t \varphi_\mathrm{e}(\boldsymbol{x},\eta)\,\frac{d\eta}{\tau} , \tag{18}$$

where $\psi(\boldsymbol{x},0) = 0$ corresponds to the unburned initial condition. The amount of heat is proportional to the increasing of the fuel temperature $T(\boldsymbol{x},t)$, with $T(\boldsymbol{x},0) = T_\mathrm{a}(\boldsymbol{x})$, then

$$\psi(\boldsymbol{x},t) \propto \frac{T(\boldsymbol{x},t) - T_\mathrm{a}(\boldsymbol{x})}{T_\mathrm{ign} - T_\mathrm{a}(\boldsymbol{x})} , \tag{19}$$

where T_ign is the ignition temperature. Hence, by replacing into Eq. (19) for simplicity the proportionality, i.e. $\propto$, with the equality, i.e. $=$, when $\psi(\boldsymbol{x},t) = 1$ in points $\boldsymbol{x} \in \Omega'(t)$ the ignition occurs and fire goes on according to (12) by setting $\mathcal{I}_{\Omega'}(\boldsymbol{x},t) = 1$.

To conclude, in this framework the temperature field emerges to be established by the following equation

$$\frac{\partial T(\boldsymbol{x},t)}{\partial t} = \varphi_\mathrm{e}(\boldsymbol{x},t)\,\frac{T_\mathrm{ign} - T_\mathrm{a}(\boldsymbol{x})}{\tau} . T \le T_\mathrm{ign} , \tag{20}$$

If $T_\mathrm{a}(\boldsymbol{x}) = T_\mathrm{a} = \mathrm{constant}$, after using (15) Eq. (20) becomes the following reaction-diffusion type equation

$$\frac{\partial T}{\partial t} = \mathcal{E}T + \frac{T_\mathrm{ign} - T_\mathrm{a}}{\tau}\left\{\mathcal{I}_{\Omega_0}(\boldsymbol{x}) + \mathcal{W}(\boldsymbol{x},t)\right\} , \tag{21}$$

NHESSD
1, 6521–6557, 2013
Modelling wildland fire propagation
G. Pagnini and A. Mentrelli

where the identity $\varphi_e(\boldsymbol{x},0) = \mathcal{I}_{\Omega_0}(\boldsymbol{x})$ is used and

$$\mathcal{W}(\boldsymbol{x},t) = \int_0^t \left\{ \int_{\Omega(\theta)} \nabla_{\overline{\boldsymbol{x}}} \cdot [\boldsymbol{V}(\overline{\boldsymbol{x}},\theta) f(\boldsymbol{x};\theta|\overline{\boldsymbol{x}})] \, d\overline{\boldsymbol{x}} \right\} d\theta \, . \tag{22}$$

4 Model discussion

The random trajectory of each active flame holder is determined as $\boldsymbol{X}^{\omega}(t,\boldsymbol{x}) = \overline{\boldsymbol{x}}_{\text{ROS}} + \chi^{\omega} + \xi^{\omega}$ where $\overline{\boldsymbol{x}}_{\text{ROS}}$ is a deterministic position driven by the ROS according to (3) and χ and ξ are the noises corresponding to turbulence and fire spotting, respectively.

The modelling of random processes in wildland fire propagation is embodied by the PDF $f(\boldsymbol{x};t|\overline{\boldsymbol{x}})$ accounting for the two independent random variables: $(\overline{\boldsymbol{x}}+\chi)$ and ξ, which represent turbulence and fire spotting, respectively. The PDF f is thus, in general, the convolution of the PDF associated to $(\overline{\boldsymbol{x}}+\chi)$, hereinafter labelled as G, and the one associated to ξ, hereinafter labelled as q. Some remarks are in order:

- Embers are carried by the atmospheric mean wind $\boldsymbol{U}$ and they land at a certain distance ℓ from the fireline along the mean wind direction $\hat{\boldsymbol{n}}_U$. Hence, the effect of the fire spotting noise ξ is always aligned with the mean wind direction $\hat{\boldsymbol{n}}_U$, i.e. $\xi^{\omega} = \ell^{\omega}\,\hat{\boldsymbol{n}}_U$. Moreover, turbulent noise χ is a zero-mean noise, i.e. $\langle\chi\rangle = 0$, while fire spotting noise ξ has a positive mean value, i.e. $\langle\ell\rangle > 0$, the mean wind velocity $\boldsymbol{U}$ being the same in all realizations. Finally, the average position in the leeward sector is $\langle\boldsymbol{X}(t,\overline{\boldsymbol{x}}_0)\rangle = \overline{\boldsymbol{x}} = \overline{\boldsymbol{x}}_{\text{ROS}} + \langle\ell\rangle\,\hat{\boldsymbol{n}}_U$ while in the windward sector is $\langle\boldsymbol{X}(t,\overline{\boldsymbol{x}}_0)\rangle = \overline{\boldsymbol{x}} = \overline{\boldsymbol{x}}_{\text{ROS}}$.

- It is also observed that fire spotting is an intrinsically downwind-phenomenon. This means that the effect of fire spotting has to be taken into account only in the

NHESSD
1, 6521–6557, 2013

Modelling wildland fire propagation

G. Pagnini and A. Mentrelli

leeward part of the fireline:

$$f(\boldsymbol{x};t|\overline{\boldsymbol{x}}) = \begin{cases} \int_0^\infty G(\boldsymbol{x}-\overline{\boldsymbol{x}}-\ell\,\hat{\boldsymbol{n}}_U;t)\,q(\ell;t)\,d\ell\,, & \text{if} \quad \hat{\boldsymbol{n}}\cdot\hat{\boldsymbol{n}}_U \geq 0 \\ G(\boldsymbol{x}-\overline{\boldsymbol{x}};t)\,, & \text{otherwise} \end{cases}, \tag{23}$$

The turbulent diffusion model can be derived by considering the scalar conservation equation. The model is determined by assuming a parameterization of the turbulent heat fluxes. The most simple model is the Gaussian one that, in the isotropic case, is

$$G(\boldsymbol{x}-\overline{\boldsymbol{x}};t) = \frac{1}{2\pi\sigma^2(t)}\exp\left\{-\frac{(x-\overline{x})^2+(y-\overline{y})^2}{2\,\sigma^2(t)}\right\}, \tag{24}$$

where $\boldsymbol{x}\equiv(x,y)$, $\overline{\boldsymbol{x}}\equiv(\overline{x},\overline{y})$, and $\sigma^2(t)=\langle(\boldsymbol{x}-\overline{\boldsymbol{x}})^2\rangle/2$ is the particle displacement variance which is related to the turbulent diffusion coefficient $\mathcal{D}_\mathrm{T}$ by the law $\sigma^2(t) = 2\mathcal{D}_\mathrm{T}\,t$. In the present model, which is oversimplified because mainly intended to investigate the potentiality of the proposed approach, the whole effect from turbulent processes with different scales, i.e. from the Atmospheric Boundary Layer to the fire-induced flow, is assumed to be parameterized by the turbulent diffusion coefficient $\mathcal{D}_\mathrm{T}$ only.

The determination of the PDF of the downwind distribution of firebrands has been studied by numerical solution of balance equations (Sardoy et al., 2008; Kortas et al., 2009). Sardoy et al. (2008) obtained that the phenomenon follows a bimodal distribution, but solely the firebrands with short-distance landing were considered important for the analysis of danger related to fire spotting, since they have the potential to ignite a new fire, while those with a long-distance landing reach the ground in a char oxidation state. Hence, here-long distance landing distribution is neglected. Furthermore, the frequency of the landing distance significantly increases with the separation from the source and, after a maximum value, gently decreases towards a minimum. In particular it has been argued (Sardoy et al., 2008) that it follows a log-normal distribution:

$$q(\ell;t) = \frac{1}{\sqrt{2\pi}\, s(t)\, \ell} \exp\left\{-\frac{(\ln \ell - \mu(t))^2}{2\, s(t)^2}\right\}, \tag{25}$$

where $\mu(t) = \langle \ln \ell \rangle$ and $s(t) = \langle (\ln \ell - \mu(t))^2 \rangle$ are, respectively, the mean and the standard deviation of $\ln \ell$. Another possible choice for q (Kortas et al., 2009) is the Weibull distribution:

$$q(\ell;t) = \frac{h}{\lambda(t)} \left(\frac{\ell}{\lambda(t)}\right)^{h-1} \exp\left\{-\left(\frac{\ell}{\lambda(t)}\right)^{h}\right\}, \tag{26}$$

where h, which depends on the firebrand shape, is established by experimental validation, and the mean value $\langle \ell \rangle$ is determined as $\langle \ell \rangle = \int_0^\infty \ell\, q(\ell;t)\, d\ell = \lambda\, \Gamma\left(1 + 1/h\right)$. When $h = 2$, the Weibull distribution becomes the Rayleigh distribution, that has been used for theoretical modelling (Wang, 2011).

The effects of turbulence into the present wildland fire propagation approach have been previously discussed (Pagnini and Massidda, 2012, 2013). If solely turbulence is considered, the mean fireline position $\langle \boldsymbol{X}(t, \overline{\boldsymbol{x}}_0) \rangle$ remains the same as determined by the level-set method, and than established according to the ROS $\mathcal{V}(\boldsymbol{x}, t)$, i.e. $\langle \boldsymbol{X}(t, \overline{\boldsymbol{x}}_0) \rangle = \overline{\boldsymbol{x}}(t) = \overline{\boldsymbol{x}}_{\mathrm{ROS}}(t)$ because $\langle \chi \rangle = 0$. For a plane front ($\kappa = 0$), when the heating-before-burning mechanism is not taken into account and the threshold value $\varphi_{\mathrm{e}}^{\mathrm{th}} = 0.5$ is assumed, it has been noted that the burned area Ω_e grows slower than that determined by the level-set method (Pagnini and Massidda, 2013). Instead, when pre-heating is considered, the advancement of the front is faster (Pagnini and Massidda, 2013). Moreover, by taking into account turbulence also the fire flank and backing fire phenomena are modelled (Pagnini and Massidda, 2013).

NHESSD
1, 6521–6557, 2013

When the contribution by fire spotting is taken into account, i.e. in the leeward fireline sector, it is easily seen that the advancement of the fireline is enhanced:

$$\begin{aligned}\langle \boldsymbol{X}(t,\overline{\boldsymbol{x}}_0)\rangle = \overline{\boldsymbol{x}}(t) &= \overline{\boldsymbol{x}}_{\mathrm{ROS}}(t) + \langle \chi \rangle + \langle \xi \rangle \\ &= \overline{\boldsymbol{x}}_{\mathrm{ROS}}(t) + \langle \ell(t) \rangle \, \hat{\boldsymbol{n}}_U \,, \end{aligned} \tag{27}$$

since $\langle \ell(t) \rangle > 0$ and $\hat{\boldsymbol{n}}_U$ is a unit vector pointing outward of the burned domain, i.e. $\hat{\boldsymbol{n}} \cdot \hat{\boldsymbol{n}}_U > 0$. As a consequence, when the fire spotting is included, the velocity of the mean fireline progression in the leeward sector is higher than the ROS, i.e.

$$\begin{aligned}\boldsymbol{V}(\overline{\boldsymbol{x}},t) = \frac{d\overline{\boldsymbol{x}}}{dt} &= \frac{d}{dt}(\overline{\boldsymbol{x}}_{\mathrm{ROS}}(t) + \langle \ell \rangle \, \hat{\boldsymbol{n}}_U) \\ &= \mathcal{V}_{\mathrm{ROS}}(\overline{\boldsymbol{x}},t)\,\hat{\boldsymbol{n}} + \frac{d\langle \ell \rangle}{dt}\,\hat{\boldsymbol{n}}_U + \langle \ell \rangle \frac{d\hat{\boldsymbol{n}}_U}{dt} \\ &= \boldsymbol{V}_{\mathrm{ROS}}(\overline{\boldsymbol{x}},t) + \boldsymbol{V}_{\ell}(\overline{\boldsymbol{x}},t)\,. \end{aligned} \tag{28}$$

The above result, expressed by Eq. (28), is a key feature of the proposed approach because it determines the correction $\boldsymbol{V}_{\ell}(\overline{\boldsymbol{x}},t)$ due to the fire spotting phenomenon that affects the fireline velocity. The latter, in fact, is generally assumed to include only the ROS contribution, i.e. $\boldsymbol{V}_{\mathrm{ROS}}(\overline{\boldsymbol{x}},t) = \mathcal{V}_{\mathrm{ROS}}(\boldsymbol{x},t)\,\hat{\boldsymbol{n}}$. It is here remarked that the new additional terms appearing in Eq. (28) are independent of the procedure for the determination of the ROS and the level-set equation for the leeward sector turns out to be

$$\frac{\partial \gamma}{\partial t} = (\mathcal{V}_{\mathrm{ROS}} + \boldsymbol{V}_{\ell} \cdot \hat{\boldsymbol{n}}) \|\nabla \gamma\| \,. \tag{29}$$

Another important result of the proposed approach is the possibility to manage real world cases in which fire overcomes a zone without fuel, like roads, firebreak lines, rivers. This valuable feature of the model has also been observed in the case in which only turbulence was taken into account (Pagnini and Massidda, 2012, 2013). In opposition, in the classical level-set method this issue cannot be solved, because

NHESSD
1, 6521–6557, 2013

G. Pagnini and A. Mentrelli

when there is no fuel the velocity field is null too, i.e. $\boldsymbol{V}(\boldsymbol{x},t) = 0$, and the fire front stops. Indeed, when the fuel is null the fireline spreading is driven by the action of the turbulent motion of the hot air and, in the leeward sector of the fireline, also by the presence of embers carried by the wind. Hence, the fire propagates according to the following diffusion-type equation following from 16 by setting $\boldsymbol{V}(\boldsymbol{x},t) = 0$, i.e.

$$\frac{\partial \varphi_e}{\partial t} = \mathcal{E}\,\varphi_e\,. \tag{30}$$

5 Numerical results

The modelling approach qualitatively discussed in the previous section, is now quantitatively analyzed by means of numerical simulations. To this purpose, a C/OpenMP code has been developed starting from a C code previously developed and successfully employed for the analysis of the turbulence effects by Pagnini and Massidda (2013, 2012). The present code, still under active development and thoroughly described elsewhere in future, aims at being a general-purpose code allowing for the simulation of wildfire propagation under a large variety of atmospheric and environmental conditions, including realistic fire-breaks and air flow fields (wind) of practical interest.

Since the aim of the present paper is to investigate the potentialities of the model discussed in the previous section, rather than simulate a wildland fire under realistic conditions, the numerical results presented in the following are restricted to oversimplified cases suitable to highlight some of the main features of the model. To this purpose, the results obtained with the full-featured model are compared to those obtained in the absence of the fire spotting effects as well as to those obtained adopting the classical approach involving a deterministic front propagation (i.e. with the classical level-set method). Moreover, the test cases are also chosen in a way as to facilitate the comparison with results available in the literature, obtained by means of different approaches.

NHESSD
1, 6521–6557, 2013

5.1 Simulation set-up

Among the variety of wildland fire phenomenology that the numerical code permits to simulate, a fireline propagating in a flat terrain covered by an idealised *Pinus ponderosa* ecosystem has been selected, following previous analysis on the same issues (Sardoy et al., 2007, 2008; Perryman et al., 2013).

The initial fireline Γ_0 is assumed to be circular, and the maximum value of the rate of spread (ROS), $\mathcal{V}_0$, is estimated by means of the Byram formula (Byram, 1959; Alexander, 1982):

$$\mathcal{V}_0 = \frac{I}{H \omega_0} , \tag{31}$$

where I is the surface fireline intensity, H is the fuel low heat of combustion and ω_0 is the oven-dry mass of fuel consumed per unit area in the active flaming zone (all the numerical values are given in Tables 1 and 2).

The functional dependence of the ROS on the wind and on the terrain slope is taken into account through two corrective factors, f_W and f_S, respectively for the wind and slope effects, which are computed following the prescription of the fireLib and Fire Behaviour SDK libraries (http://fire.org; see also Mandel et al., 2011), in the case of the NFFL (Northern Forest Fire Laboratory) Model 9. As to guarantee that upon application of the corrective factors f_W and f_S, the maximum ROS, i.e. the ROS corresponding to the worst-case scenario, equals the ROS prescribed by the Byram formula, $\mathcal{V}_0$, a suitable factor α is also introduced. As a result, the formula for the ROS reads as follows:

$$\mathcal{V}(\boldsymbol{x}, t) = \mathcal{V}_0 \, \frac{(1 + f_W + f_S)}{\alpha} , \tag{32}$$

The mean wind is assumed to be constant both in direction, $\hat{\boldsymbol{n}}$, and velocity, U_t, in order to highlight the effects of the fire spotting. In particular, in all the plotted results the wind is directed along the positive x direction (i.e. $\hat{\boldsymbol{n}} \equiv \hat{\boldsymbol{i}}$) and the wind velocity, U_t, is intended as the velocity at the top of the tree canopy which, following Sardoy et al. (2008), is assumed to be equal to 10 m.

The turbulent heat transfer is modelled by means of the Gaussian distribution, see Eq. (24), and firebrand landing is modelled, following Sardoy et al. (2007, 2008), by means of a log-normal distribution, as given in Eq. (25). In order to focus on the effects of the fire spotting phenomena, the turbulent diffusion coefficient $\mathcal{D}_T$ is assumed to be constant throughout the numerical simulations, as well as the ignition delays of the hot air and of the firebrands. In particular, it is well-known that the value of thermal diffusity in air is around $2 \times 10^{-5}\,\mathrm{m^2\,s^{-1}}$, then the effect of turbulence is here accounted for generating a turbulent diffusion coefficient of three orders of magnitude higher, i.e. $\mathcal{D}_T = 4 \times 10^{-2}\,\mathrm{m^2\,s^{-1}}$. This value has been chosen also in view of the analysis of the role and the effects of firebrands. A more detailed study of turbulence effects with higher value of $\mathcal{D}_T$ has been performed by Pagnini and Massidda (2013, 2012). All the chosen values are given in Table 1.

Concerning fire spotting modelling, Sardoy et al. (2008) distinguish two landing regimes according to the Froude Number $Fr = U_t / \sqrt{g L_c}$, where g is the gravitation acceleration and L_c is the characteristic length of the plume convecting embers, calculated by $L_c = \left(I / \left(\rho_\infty c_{pg} T_a \sqrt{g}\right)\right)^{2/3}$, where ρ_∞, T_a and c_{pg} are, respectively, the ambient gas density and temperature and the specific heat of gas. The two mentioned regimes are: the buoyancy-driven regime ($Fr < 1$), and the wind-driven regime ($Fr > 1$). In particular, following the fitting of numerical data generated by Sardoy et al. (2008) when the char content is $\nu_c = 0.39$, Perryman et al. (2013) suggest the following pairs of parameters:

– buoyancy-driven regime ($Fr < 1$)

$$\mu = 1.47\, I_f^{0.54}\, U_t^{-0.55} + 1.14, \tag{33a}$$

$$s = 0.86\, I_f^{-0.21}\, U_t^{0.44} + 0.19, \tag{33b}$$

NHESSD
1, 6521–6557, 2013

Modelling wildland fire propagation

G. Pagnini and A. Mentrelli

– wind-driven regime ($Fr > 1$)

$$\mu = 1.32\, I_f^{0.26}\, U_t^{0.11} - 0.02, \tag{34a}$$

$$s = 4.95\, I_f^{-0.01}\, U_t^{-0.02} - 3.48, \tag{34b}$$

where U_t must be given in m s^{-1} and I_f, given in kW m^{-1}, represents the fire intensity enriched by tree torching intensity I_t, i.e. $I_f = I + I_t$.

It is well-known that, in the log-normal density, to the increasing of the value of the mean μ corresponds a slower decay of the right-tail, i.e. for $\ell \to \infty$, and correspondingly a faster decay for the left-tail, i.e.$\ell \to 0$, which it means an higher probability to have large value of ℓ. Indeed, to an increasing of the value of the standard deviation s corresponds a left-shift of the maximum value of the probability density, which it means that the most frequent event has a small value of ℓ.

As previously pointed out, simulations are performed following some of the case studies considered by other authors, in particular by Sardoy et al. (2008). With the purpose of pointing out the main features of the model proposed here, four cases have been regarded as worth of discussion; these four cases correspond to the possible combinations of two selected values of the fire intensity I and two selected values of the mean wind velocity U_t (I = 10 000–30 000 kW m^{-1}; U_t = 6.7–17.88 m s^{-1}). In Table 2, these four cases (named as case $\mathcal{A}$, $\mathcal{B}$, $\mathcal{C}$ and $\mathcal{D}$) are properly defined.

As mentioned earlier, in all the four cases under investigation, numerical simulations have been performed assuming a deterministic front propagation, i.e. neglecting turbulence and the fire spotting phenomenon, and assuming a random front propagating both in presence and absence of fire spotting phenomenon.

Moreover, in all cases, simulations have been carried out assuming that the wildland fire freely propagates on the flat terrain, as well as introducing two fire-breaks, the latter being modelled as two combustible-free stripes of terrain perpendicular to the wind direction located windward and leeward with respect to the initial fire location.

As a result, for each of the four test cases, the results of a set of six numerical simulations are presented and collectively discussed.

5.2 Discussion

The results of the numerical simulations corresponding to the four cases previously introduced and summarized in Table 2 are shown in Figs. 1, 2, 3 and 4, respectively.

In each of the figures, the evolutions of the fireline freely propagating in a terrain with no fire-breaks (i.e. fuel-free regions) are shown on the left, and the corresponding evolution in presence of two fire-breaks is shown on the right, being the fire-breaks represented by grey vertical, i.e. perpendicular to the wind direction, stripes of different width (see Table 1 for the values of all the model parameters). For both cases (without and with fire-breaks), the results obtained by adopting three different models are shown in the figures: the deterministic model, in which the firefront is tracked by means of the classical level-set method (top raw of each figure); the model in which the front is tracked by means of the randomized level-set method including only the turbulence effects (middle raw), and the full-featured model presented in the previous section in which the fire spotting phenomenon is also included (bottom raw).

In general, it is possible to note the high number, the variability and the complexity of phenomenological situations that the present approach can handle, as well as the strong sensibility to different framework features.

As a general rule, by comparison of the results obtained in the randomized approach to those obtained in the deterministic framework, it is possible to state that, as expected, the firefront propagates faster when turbulence effects are taken into account. Moreover, when fire spotting effects are also included in the model, the firefront propagates even faster, if compared with results obtained with the model including only the turbulence effects. These results, sensibly appreciable in all the four cases proposed in Figs. 1, 2, 3 and 4, are a consequence of the air pre-heating action due to the turbulent heat transfer mechanism (a phenomenon enhanced by turbulence) and of the rapid burning mechanism connected to the ember landing in a yet-to-burn region standing in front of the fireline (a phenomenon peculiar to fire spotting).

Moreover, fire flanking and backing fire appear well simulated.

NHESSD
1, 6521–6557, 2013

Even though it should be remarked that the purpose of this analysis is limited to a first-look investigation of the capabilities of the model, and no attempt has been made in order to chose the model parameters in a realistic way, still the effects of the fire spotting phenomenon appear relevant and worthy of being taken into account in any model aiming at the realistic simulation of the behaviour of wildland fire.

The presented numerical results, in fact, strongly support the importance of the fire spotting phenomenon as a mechanism enhancing the frontline propagation: This is particularly evident in the cases in which the fire propagates in a region in which fire-breaks are present. In this situation, the modelling results strikingly point out how the fire spotting phenomenon may be crucial in making the fire overcoming the fire-breaks faster than when adopting a model including only turbulence effects. As it has been previously shown (Pagnini and Massidda, 2013, 2012), the turbulence itself can be responsible for the spreading of the wildland fire across fire-breaks; but it appears clearly, when comparing the results of Figs. 1d, 2d, 3d and 4d to the corresponfing ones of Figs. 1f, 2f, 3f and 4f, that the fire spotting phenomenon is capable of remarkably enhancing this capability of the wildland fire. It is worth noting here that, since the present analysis is primarily devoted to the investigation of the main feature of the new model including fire spotting effects, the numerical results are presented for *short-time* propagation of the fire, in contrast to the results discussed in Pagnini and Massidda (2013) in which, being the focus of the analysis on the turbulence effects, the numerical results concerned *long-term* propagation. In a long-term analysis, the simulation results presented in Figs. 1d, 2d, 3d and 4d would show that the fire is capable of overcoming the fire-breaks solely due to heating mechanism connected to turbulence, but it is stressed here that the fire spotting can greatly improve this capability of the firefront.

NHESSD
1, 6521–6557, 2013

6 Conclusions

An approach for tracking random fronts (Pagnini and Bonomi, 2011; Pagnini and Massidda, 2013, 2012) has been described, re-arranged and analyzed to study its suitability to investigate the effects of random processes on wildland fire propagation. Actually, the random fireline is modelled in terms of an average position determined by a level-set model with a certain ROS and the statistical spread is determined by the PDF of displacements of random-contour points marked as *active* flame holders.

This formulation is similar to the so-called SPH theory (Monaghan, 2005) where a kernel function with a smoothing length is introduced to study non-smooth solutions. In the present approach, non-smooth solutions obtained by the level-set equation are weighted by a kernel function with a smoothing length that straightforwardly follows to be determined by the PDF of contour points.

This approach is a generalization of the level-set method that permits to track even random fronts and the effective fireline contours emerges to be governed by a reaction-diffusion type equation. This last fact reconciles the two largely used approaches to study wildland fire propagation, namely that one based on the level-set method with a given ROS and that based on reaction-diffusion equations.

In previous analysis (Pagnini and Massidda, 2013, 2012) only turbulence effects were considered. Here, also random effects due to the fire spotting phenomenon has been taken into account. In this respect, in order to consider the statistical effect due to fire spotting, a formula is stated to modify the velocity of the average frontline driven by the level-set equation.

Numerical simulations of a simple case study are performed to explore the model behaviour. Fire spotting parameterization follows numerical results by Sardoy et al. (2008) combined with argouments by Perryman et al. (2013) and the maximum value of the ROS has been estimated by Byram formula (Byram, 1959; Alexander, 1982). The values for turbulent diffusion coefficient and ignition delay have been opportunely

NHESSD
1, 6521–6557, 2013

G. Pagnini and A. Mentrelli

Title Page
Abstract | Introduction
Conclusions | References
Tables | Figures
◂◂ | ▸▸
◂ | ▸
Back | Close
Full Screen / Esc
Printer-friendly Version
Interactive Discussion

chosen to better highlight the role of each single phenomenon and the structure of their joined action.

In particular, for the same given ROS, the model shows a faster fireline propagation with respect to the level-set formulation and, in opposition to the level-set based modelling, the randomization permits to model backing fire, fire flanking and fire overcaming an obstacle without fuel.

The presence of fire spotting leads the fireline to be faster in the leeward sector than in the windward sector which is affected solely by turbulence. Moreover, a shortest ignition delay is associated to fire spotting because of its burning by contact rather than by heating. This fact generates a further increasing of propagation speed in the downwind direction.

The role of the fire intensity and of the mean wind are also analyzed. The effect due to the increasing of the fire intensity emerges to be stronger than that due to the increasing of the mean wind to propagate faster the fire. This is a direct consequence of the ROS estimation.

To conclude, this formulation emerges to be more suitable than the ordinary level-set approach to manage real world dangerous situations related to the random character of wildland fire propagation. In fact, this modelling approach allows to predict fire flanking, backing fire, fire faster propagation as a consequence of the pre-heating action by the hot air and of the firebrand landing and it has the paramount property to reproduce the overcoming of a break-fire without fuel by the fire because of the diffusion of the hot air (Pagnini and Massidda, 2013, 2012) and ember jumping. The validation of the present modelling approach with realistic parameters of turbulence and ignition delay will be the topic of a further furture research.

NHESSD
1, 6521–6557, 2013

References

Alexander, M. E.: Calculating and interpreting forest fire intensities, Can. J. Bot., 60, 349–357, 1982. 6540, 6545

Almeida, R. M. and Macau, E. E. N.: Stochastic cellular automata model for wildland fire spread dynamics, J. Phys. Conf. Ser., 285, 012038, 2011. 6524

Asensio, M. I. and Ferragut, L.: On a wildland fire model with radiation, Int. J. Numer. Meth. Engng., 54, 137–157, 2002. 6523, 6525

Babak, P., Bourlioux, A., and Hillen, T.: The effect of wind on the propagation of an idealized forest fire, SIAM J. Appl. Math., 70, 1364–1388, 2009. 6523, 6525

Balbi, J. H., Rossi, J. L., Marcelli, T., and Santoni, P. A.: A 3D physical real-time model of surface fires across fuel beds, Combust. Sci. Technol., 179, 2511–2537, 2007. 6528, 6533

Balbi, J. H., Morandini, F., Silvani, X., Filippi, J. B., and Rinieri, F.: A physical model for wildland fires, Combust. Flame, 156, 2217–2230, 2009. 6528, 6533

Beezley, J. D., Chakraborty, S., Coen, J. L., Douglas, C. C., Mandel, J., Vodacek, A., and Wang, Z.: Real-Time Data Driven Wildland Fire Modeling, in: Computational Science, ICCS 2008, 8th International Conference, Kraków, Poland, 23–25 June 2008, Proceedings, Part III, edited by: Bubak, M., van Albada, G. D., Dongarra, J., and Sloot, P. M. A., Lect. Notes Comput. Sci., 5103, 46–53, Springer, Berlin, Heidelberg, 2008. 6526

Boychuk, D., Braun, W. J., Kulperger, R. J., Krougly, Z. L., and Stanford, D. A.: A stochastic forest fire growth model, Environ. Ecol. Stat., 16, 133–151, 2009. 6524

Byram, G. M.: Combustion of forest fuels, in: Forest Fire: Control and Use, edited by: Davis, K. P., 61–89, McGraw Hill, New York, 1959. 6540, 6545

Clark, T. L., Jenkins, M. A., Coen, J., and Packham, D.: A coupled atmospheric-fire model: convective feedback on fire-line dynamics, J. Appl. Meteor., 35, 875–901, 1996. 6524

Clements, C. B., Zhong, S., Bian, X., Heilman, W. E., and Byun, D. W.: First observations of turbulence generated by grass fires, J. Geophys. Res., 113, D22102, doi:10.1029/2008JD010014, 2008. 6524

Coen, J. J., Cameron, M., Michalakes, J., Patton, E. G., Riggan, P. J., and Yedinak, K. M.: WRF-Fire: coupled weather-wildland fire modeling with the Weather Research and Forecasting model, J. Appl. Meteor. Climatol., 52, 16–38, 2013. 6526, 6528

Cunningham, P. and Linn, R. R.: Numerical simulations of grass fires using a coupled atmosphere-fire model: dynamics of fire spread, J. Geophys. Res., 112, D05108, 2007. 6524

Dobrinkova, N., Jordanov, G., and Mandel, J.: WRF-Fire Applied in Bulgaria, in: Numerical Methods and Applications, NMA 2010, 7th International Conference, Borovets, Bulgaria, 20–24 August 2010, edited by: Dimov, I., Dimova, S., and Kolkovska, N., Lect. Notes Comput. Sc., 6046, 133–140, Springer, Berlin, Heidelberg, 2011. 6526

Favier, C.: Percolation model of fire dynamic, Phys. Lett. A, 330, 396–401, 2004. 6524

Filippi, J. B., Bosseur, F., Mari, C., Lac, C., Moigne, P. L., Cuenot, B., Veynante, D., Cariolle, D., and Balbi, J. H.: Coupled atmosphere-wildland fire modelling, J. Adv. Model. Earth Syst., 1, art. #11, 2009. 6524

Filippi, J. B., Morandini, F., Balbi, J. H., and Hill, D.: Discrete event front tracking simulator of a physical fire spread model, Simulation, 86, 629–646, 2010. 6529

Filippi, J. B., Bosseur, F., Pialat, X., Santoni, P. A., Strada, S., and Mari, C.: Simulation of coupled Fire/Atmosphere interaction with the MesoNH-ForeFire models, J. Combust., 2011, 540390, doi:10.1155/2011/540390, 2011. 6524

Filippi, J. B., Pialat, X., and Clements, C. B.: Assessment of ForeFire/Meso-NH for wildland fire/atmosphere coupled simulation of the FireFlux experiment, Proc. Combust. Inst., 34, 2633–2640, 2013. 6524, 6529

Finney, M.: Fire growth using minimum travel time methods, Can. J. For. Res., 32, 420–1424, 2002. 6528, 6533

Finney, M.: Calculation of fire spread rates across random landscapes, Int. J. Wildland Fire, 12, 167–174, 2003. 6528, 6533

Forthofer, J. M. and Goodrick, S. L.: Review of vortices in wildland fire, J. Combust., 2011, 984363, 2011. 6524

Hunt, H.: A new conceptual model for forest fires based on percolation theory, Complexity, 13, 12–17, 2007. 6524

Klimontovich, Y. L.: Nonlinear Brownian motion, Phys.-Uspekh., 37, 737–767, 1994. 6529

Koo, E., Pagni, P. J., Weise, D. R., and Woycheese, J. P.: Firebrands and spotting ignition in large-scale fires, Int. J. Wildland Fire, 19, 818–843, 2010. 6524

Kortas, S., Mindykowski, P., Consalvi, J. L., Mhiri, H., and Porterie, B.: Experimental validation of a numerical model for the transport of firebrands, Fire Safety J., 44, 1095–1102, 2009. 6524, 6536, 6537

Linn, R. R. and Cunningham, P.: Numerical simulations of grass fires using a coupled atmosphere-fire model: Basic fire behavior and dependence on wind speed, J. Geophys. Res., 110, D13107, doi:10.1029/2004JD005597, 2005. 6524

Mallet, V., Keyes, D. E., and Fendell, F. E.: Modeling wildland fire propagation with level set methods, Comput. Math. Appl., 57, 1089–1101, 2009. 6523, 6526, 6528, 6533

Mandel, J., Bennethum, L. S., Beezley, J. D., Coen, J. L., Douglas, C. C., Kim, M., and Vodacek, A.: A wildland fire model with data assimilation, Math. Comput. Simulat., 79, 584–606, 2008. 6523, 6525, 6526

Mandel, J., Beezley, J. D., Coen, J. L., and Kim, M.: Data assimilation for wildland fires: Ensemble Kalman filters in coupled atmosphere-surface models, IEEE Control. Sys. Mag., 29, 47–65, 2009. 6526, 6528

Mandel, J., Beezley, J. D., and Kochanski, A. K.: Coupled atmosphere-wildland fire modeling with WRF 3.3 and SFIRE 2011, Geosci. Model Dev., 4, 591–610, doi:10.5194/gmd-4-591-2011, 2011. 6523, 6524, 6526, 6528, 6540

Monaghan, J. J.: Smoothed particle hydrodynamics, Rep. Prog. Phys., 68, 1703–1759, 2005. 6532, 6545

Montenegro, R., Plaza, A., Ferragut, L., and Asensio, M. I.: Application of a nonlinear evolution model to fire propagation, Nonlinear Anal. Theory Methods Appl., 30, 2873–2882, 1997. 6525

Morgante, A. E.: Incorporating Spotting into a Simple Fire Perimeter Model, Master's thesis, Humboldt State University, Arcata, CA, 2011. 6524

Pagnini, G. and Bonomi, E.: Lagrangian formulation of turbulent premixed combustion, Phys. Rev. Lett., 107, 044503, doi:10.1103/PhysRevLett.107.044503, 2011. 6528, 6531, 6532, 6533, 6545

Pagnini, G. and Massidda, L.: The randomized level-set method to model turbulence effects in wildland fire propagation, in: Modelling Fire Behaviour and Risk. Proceedings of the International Conference on Fire Behaviour and Risk. ICFBR 2011, Alghero, Italy, 4–6 October 2011, edited by: Spano, D., Bacciu, V., Salis, M., and Sirca, C., 126–131, ISBN 978-88-904409-7-7, 2012. 6528, 6533, 6537, 6538, 6539, 6541, 6544, 6545, 6546

Pagnini, G. and Massidda, L.: Modelling turbulence effects in wildland fire propagation by the randomized level-set method, submitted. Conference presentation slides from the workshop "Numerical Simulation of Forest Fires, from Combustion to Emissions", Cargese (Corsica – France), 13–18 May 2013, are available here: http://forefire.univ-corse.fr/cargese2013/jeu/pagnini.pdf, 2013. 6528, 6533, 6537, 6538, 6539, 6541, 6544, 6545, 6546

Perryman, H. A.: A Mathematical Model of Spot Fires and their Management Implications, Master's thesis, Humboldt State University, Arcata, CA, 2009. 6524

NHESSD

1, 6521–6557, 2013

Modelling wildland fire propagation

G. Pagnini and A. Mentrelli

Title Page
Abstract | Introduction
Conclusions | References
Tables | Figures
◀| |▶
◀ ▶
Back | Close
Full Screen / Esc
Printer-friendly Version
Interactive Discussion

Perryman, H. A., Dugaw, C. J., Varner, J. M., and Johnson, D. L.: A cellular automata model to link surface fires to firebrand lift-off and dispersal, Int. J. Wildland Fire, 22, 428–439, 2013. 6524, 6540, 6541, 6545

Potter, B. E.: A dynamics based view of atmosphere-fire interactions, Int. J. Wildland Fire, 11, 247–255, 2002. 6524

Potter, B. E.: Atmospheric interactions with wildland fire behaviour – I. Basic surface interactions, vertical profiles and synoptic structures, Int. J. Wildland Fire, 21, 779–801, 2012a. 6524

Potter, B. E.: Atmospheric interactions with wildland fire behaviour – II. Plume and vortex dynamics, Int. J. Wildland Fire, 21, 802–817, 2012b. 6524

Rehm, R. G. and McDermott, R. J.: Fire-Front Propagation Using the Level Set Method, Tech. Note 1611, Natl. Inst. Stand. Technol., 2009. 6523, 6526

Rothermel, R. C.: A Mathematical Model for Predicting Fire Spread in Wildland Fires, Tech. Rep. Research Paper INT-115, USDA Forest Service, Intermountain Forest and Range Experiment Station, Ogden, Utah 84401, available at: http://www.treesearch.fs.fed.us/pubs/32533, 1972. 6528, 6533

Sardoy, N., Consalvi, J. L., Porterie, B., and Fernandez-Pello, A. C.: Modeling transport and combustion of firebrands from burning trees, Combust. Flame, 150, 151–169, 2007. 6524, 6540, 6541

Sardoy, N., Consalvi, J. L., Kaiss, A., Fernandez-Pello, A. C., and Porterie, B.: Numerical study of ground-level distribution of firebrands generated by line fires, Combust. Flame, 154, 478–488, 2008. 6524, 6536, 6537, 6540, 6541, 6542, 6545

Serón, F. J., Gutiérrez, D., Magallón, J., Ferragut, L., and Asensio, M. I.: The evolution of a wildland forest fire front, Visual Comput., 21, 152–169, 2005. 6525

Sethian, J. A. and Smereka, P.: Level set methods for fluid interfaces, Ann. Rev. Fluid Mech., 35, 341–372, 2003. 6523, 6526

Strada, S., Mari, C., Filippi, J. B., and Bosseur, F.: Wildfire and the atmosphere: Modelling the chemical and dynamic interactions at the regional scale, Atmos. Environ., 51, 234–249, 2012. 6523

Sullivan, A. L.: Wildland surface fire spread modelling, 1990–2007. 3: Simulation and mathematical analogue models, Int. J. Wildland Fire, 18, 387–403, 2009. 6526

Sun, R., Jenkins, M. A., Krueger, S. K., and Charney, J.: An evaluation of fire plume properties simulated with the FDS and Clark coupled wildfire model, Can. J. Forest Res., 36, 2894–2908, 2006. 6524

Sun, R., Krueger, S. K., Jenkins, M. A., Zuluar, M., and Charney, J. J.: The importance of fire-atmosphere coupling and boundary-layer turbulence to wildfire spread, Int. J. Wildland Fire, 18, 50–60, 2009. 6524

Viegas, D. X.: Forest fire propagation, Phil. Trans. R. Soc. Lond. A, 356, 2907–2928, 1998. 6523

Wang, H. H.: Analysis on downwind distribution of firebrands sourced from a wildland fire, Fire Technol., 47, 321–340, 2011. 6524, 6537

Weber, R. O., Mercer, G. N., Sidhu, H. S., and Gray, B. F.: Combustion waves for gases ($Le = 1$) and solids ($Le \to \infty$), Proc. R. Soc. Lond. A, 453, 1105–1118, 1997. 6523, 6525

Table 1. Vales of the parameters of the model which are kept fixed throughout the numerical simulation discussed here.

Fixed simulation parameters	Value
Fuel low heat of combustion, H	$22\,000\,\mathrm{kJ\,kg^{-1}}$
Oven-dry mass of fuel, ϖ_0	$2.243\,\mathrm{kg\,m^{-2}}$
Ambient gas density, ρ_∞	$1.1\,\mathrm{kg\,m^{-3}}$
Ambient gas temperature, T_a	$300\,\mathrm{K}$
Mean specific heat of gas, c_{pg}	$1\,121\,\mathrm{kJ\,(kg\,K)^{-1}}$
Gravitational acceleration, g	$9.81\,\mathrm{m\,s^{-2}}$
Tree torching intensity, I_t	$0.015\,\mathrm{kW\,m^{-1}}$
Turbulent diffusion coefficient, $\mathcal{D}_T$	$0.04\,\mathrm{m^2\,s^{-1}}$
Ignition delay of hot air, τ_h	$600\,\mathrm{s}$
Ignition delay of firebrands, τ_f	$60\,\mathrm{s}$
Width of the fire-break in the windward sector	$60\,\mathrm{m}$
Width of the fire-break in the leeward sector	$90\,\mathrm{m}$

NHESSD
1, 6521–6557, 2013

Modelling wildland fire propagation

G. Pagnini and
A. Mentrelli

Table 2. Values of the mean wind velocity, U_t, of the fire intensity, I, and of the Fr number for the four cases for which numerical results are presented here.

Case	U_t [m s^{-1}]	I [kW m^{-1}]	Fr [–]
$\mathcal{A}$	6.7	10 000	10.4
$\mathcal{B}$	6.7	30 000	7.2
$\mathcal{C}$	17.88	10 000	27.8
$\mathcal{D}$	17.88	30 000	19.3

NHESSD
1, 6521–6557, 2013

Modelling wildland fire propagation

G. Pagnini and A. Mentrelli

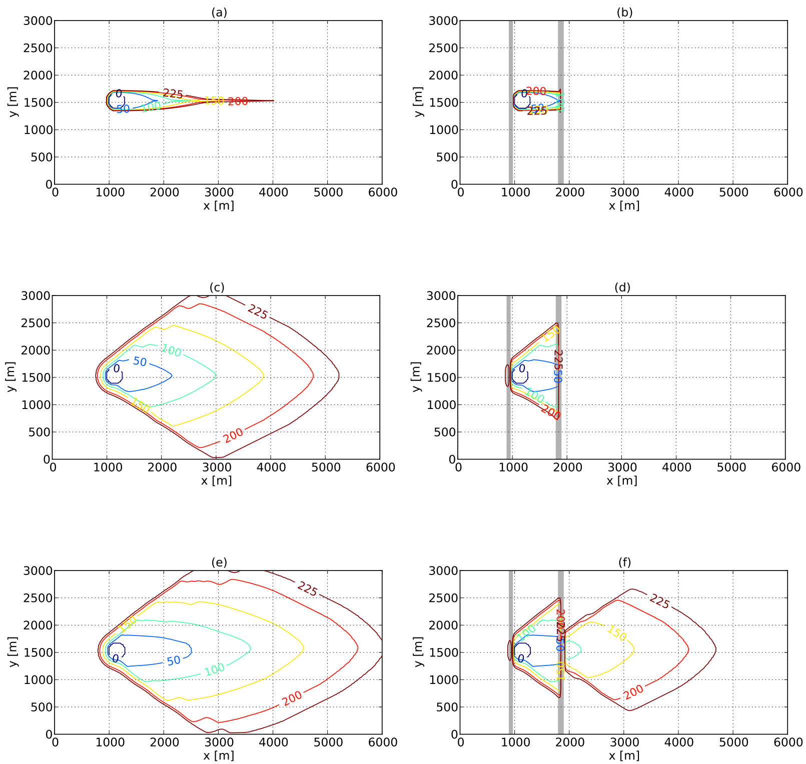

Fig. 1. Time evolution of the firefront when the mean wind velocity and the fire intensity are U_t = 6.70 m s^{-1} and I = 10 000 kW m^{-1} (case $\mathcal{A}$), in absence (on the left) and presence (on the right) of two fire-break zones (grey sripes) located on the left and on the right of the initial firefront. The results are obtained by adopting the level-set method (top row), by the present modelling approach when only turbulence is taken into account (middle raw), and when both turbulence and fire spotting are considered (bottom raw). The labels on the contour lines represent the propagation time (expressed in minutes). All the parameters of the model are given in Table 1.

NHESSD
1, 6521–6557, 2013

G. Pagnini and A. Mentrelli

Title Page
Abstract | Introduction
Conclusions | References
Tables | Figures
◀| |▶
◀ ▶
Back | Close
Full Screen / Esc
Printer-friendly Version
Interactive Discussion

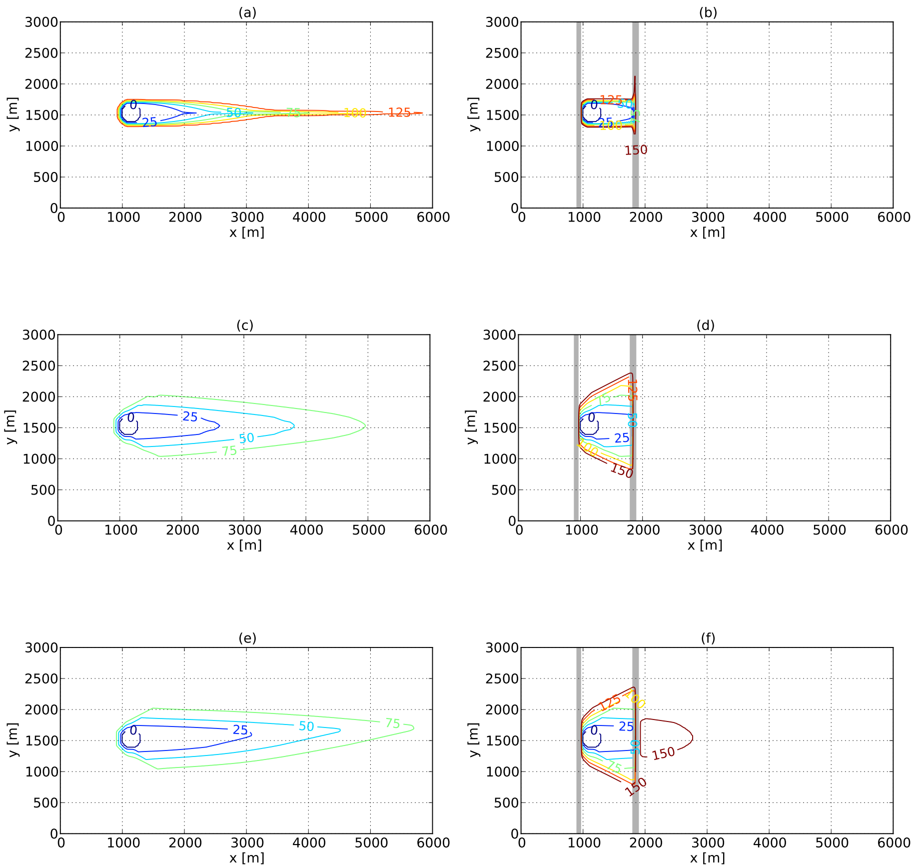

Fig. 2. The same as in Fig. 1 but when the mean wind velocity and the fire intensity are U_t = 6.70 m s^{-1} and I = 30 000 kW m^{-1} (case $\mathcal{B}$).

NHESSD
1, 6521–6557, 2013

Modelling wildland fire propagation

G. Pagnini and A. Mentrelli

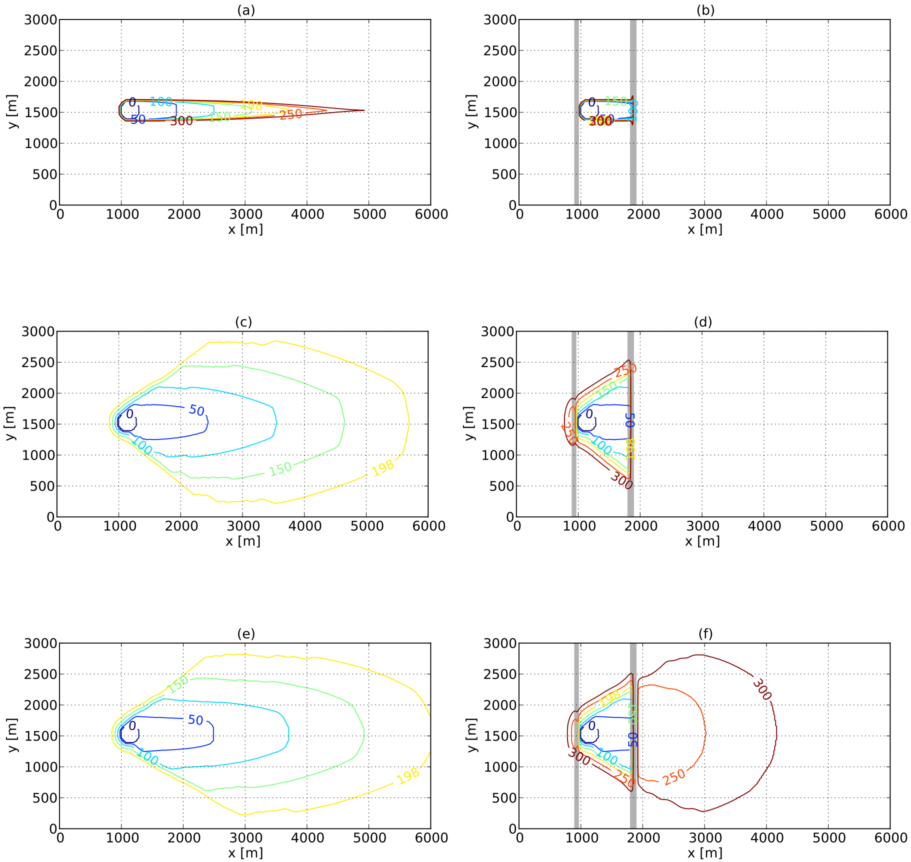

Fig. 3. The same as in Fig. 1 but when the mean wind velocity and the fire intensity are U_t = 17.88 m s^{-1} and I = 10 000 kW m^{-1} (case C).

NHESSD
1, 6521–6557, 2013

G. Pagnini and A. Mentrelli

Title Page
Abstract | Introduction
Conclusions | References
Tables | Figures
◀I | ▶I
◀ | ▶
Back | Close
Full Screen / Esc
Printer-friendly Version
Interactive Discussion

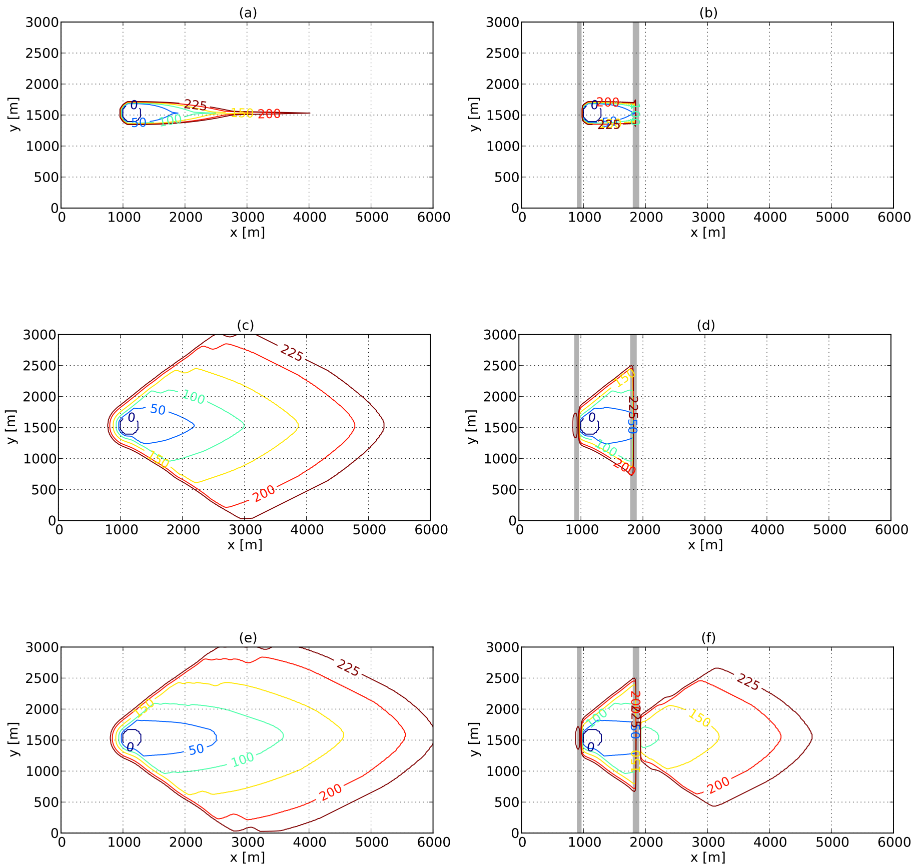

Fig. 4. The same as in Fig. 1 but when the mean wind velocity and the fire intensity are $U_t = 17.88\,\mathrm{m\,s^{-1}}$ and $I = 30\,000\,\mathrm{kW\,m^{-1}}$ (case $\mathcal{D}$).

NHESSD
1, 6521–6557, 2013